



Contents lists available at SciVerse ScienceDirect

Spectrochimica Acta Part A: Molecular and Biomolecular Spectroscopy

journal homepage: www.elsevier.com/locate/saa

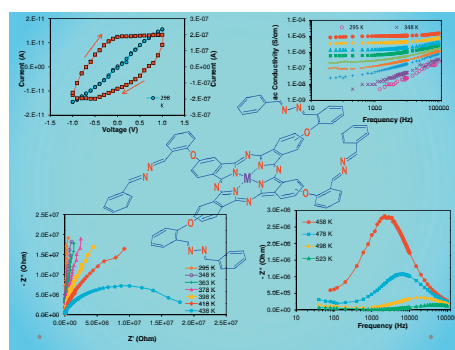
Synthesis, characterization and electrical properties of peripherally tetra-aldazine substituted novel metal free phthalocyanine and its zinc(II) and nickel(II) complexes

Rıza Bayrak^{a,*}, Fatih Dumludağ^b, Hakkı Türker Akçay^a, İsmail Değirmencioglu^a^a Department of Chemistry, Faculty of Sciences, Karadeniz Technical University, 61080 Trabzon, Turkey^b Department of Physics, Faculty of Arts and Science, Marmara University, 34722 Istanbul, Turkey

HIGHLIGHTS

- ▶ The preparation of the aldazine substituted phthalonitrile **3**.
- ▶ Synthesis and characterization of metal free **4** and metallophthalocyanines **5**, **6**.
- ▶ Dc and ac conductivity studies of the novel phthalocyanines **4–6**.

GRAPHICAL ABSTRACT



ARTICLE INFO

Article history:

Received 5 October 2012

Received in revised form 18 December 2012

Accepted 21 December 2012

Available online 2 January 2013

Keywords:

Phthalocyanine

Electrical characterization

Impedance spectra

Hopping

Semiconductor

Conductivity

ABSTRACT

The novel phthalonitrile containing azine segment and its corresponding tetra aldazine substituted metal free- and metallo-phthalocyanines (Zn(II) and Ni(II)) were synthesized and characterized by IR, ¹H NMR, Mass, UV–Vis spectroscopy and elemental analysis and addition to these techniques for substituted phthalonitrile ¹³C NMR have been used. In addition, dc and ac electrical properties of the films of these novel phthalocyanines were investigated as a function of temperature (295–523 K) and frequency (40–10⁵ Hz). Activation energy values of the films of the phthalocyanines were calculated from straight portions of the Arrhenius plot ($\ln \sigma_{dc} - 1/T$ curves) as 0.70 eV, 0.93 eV and 0.91 eV for the films of metal free, nickel- and zinc-phthalocyanines, respectively. From impedance spectroscopy measurements, it is observed that bulk resistance decreases with increasing temperature indicating semiconductor property.

© 2012 Elsevier B.V. All rights reserved.

Introduction

Phthalocyanines (Pcs) are one of the most useful heterocyclic materials. There are still many investigations on their technological applications in different scientific areas such as chemical sensors [1–3], electrochromic displaying systems [4], non-linear optics [5], solar cells [6], photo-voltaic optics, molecular electronics [7],

semiconductors [8], liquid crystals [9], optical storage devices [10], laser dyes [11], catalyst [12] and photo dynamic therapy (PDT) [13].

Phthalocyanines and their metal complex derivatives have strong delocalized π -electronic structure, good thermal stability and interesting visible area optical properties. The central cavity of Pc can complex with vary about 70 elements. Depending on specification of element; monomeric, axially ligated or dimeric phthalocyanines can be obtained. While the cations fitting central cavity of phthalocyanines form monomeric species [14], high valance and larger cations form dimeric or axially ligated species [15–17].

* Corresponding author. Tel.: +90 506 389 6589; fax: +90 462 325 3196.

E-mail address: bayrakriza@ktu.edu.tr (R. Bayrak).

Term of azine uses for description of six-membered ring system such as pyrazines, pyrimidines in heterocyclic chemistry. In acyclic chemistry, azines are synthesized that one molecule hydrazine hydrate reaction with two molecules of carbonyl compounds. Additionally this compound class is called “aldazines” when aldehyde was used as carbonyl compound [18,19]. Azines are known biological active compounds. Unsymmetrical aldazines have antitumor [20], antioxidant [21], antibacterial and antifungal activity [22–24].

In our previous work, photochemical and photophysical properties of new azine-bridged binuclear metallophthalocyanines were studied [25]. There is not any study on electrical properties of azine functionalized phthalocyanines in literature. The aim of the present work is synthesis of novel metal free-, Zn- and Ni-phthalocyanines and investigation the electrical transport properties of thin films of synthesized compounds to determine some essential parameters and predict the electronic conduction properties. In order to investigate electrical properties of the films of phthalocyanines dc and ac conductivity measurements were performed as a function of temperature (295–523 K) and frequency (40–105 Hz). Impedance spectroscopy measurements were also performed in the same temperature and frequency range.

Experimental

All reactions were carried out under dry and oxygen free nitrogen atmosphere using Schlenk system. DMF was dried and purified as described by Perrin and Armarego [26]. 2- $\{ (E)-[(2E)-(phenylmethylidene)hydrazono]methyl\}$ phenol (**1**) [27] and 4-nitrophthalonitrile (**2**) [28] was prepared according to the literature. ^1H NMR/ ^{13}C NMR spectra were recorded on a Varian XL-200 NMR spectrometer in CDCl_3 , DMSO d_6 , and chemical shifts were reported (δ) relative to MeSi_4 as internal standard. IR spectra were recorded on a Perkin–Elmer Spectrum one FT-IR spectrometer in ATR technique. The MS–MS spectrum were measured with a Thermo Quantum Access Mass spectrometer with H-ESI probe. Methanol, chloroform and acetonitrile were used as solvents in mass spectrometer and all mass analysis were conducted in positive ion mode. Elemental analysis were performed on a Costech ECS 4010 instrument, UV–Vis spectra were recorded by means of a Unicam UV2-100 spectrometer, using 1 cm pathlength cassettes at room temperature. Melting points were measured on an electrothermal apparatus and are uncorrected.

Preparation of films for electrical measurements

Interdigital transducer (IDT) was employed as transducer in order to investigate dc and ac electrical properties of the compounds. Inter digital transducers were fabricated onto glass substrate in our laboratory. The method for the fabrication of IDTs was described previously in the literature [29]. The transducer contains 21 of gold electrodes with 100 μm width. Space between the electrodes was also kept at 100 μm . In order to obtain thin film of synthesized compounds on IDT, the molecules were dissolved in chloroform using micro centrifuge tubes. The homogeny solutions were coated onto IDT using smearing method in air ambient. The substrate temperature was kept constant at 295 K during the deposition of solution onto IDT.

Electrical measurements

To investigate the electrical properties of the compounds, IDTs (coated with synthesized compounds) were placed into home-made temperature controlled aluminum chamber. Electrical contacts between electrodes and measurement chamber were done using silver paste. Dc current values were recorded by applying

dc voltages between -1 V and 1 V with 50 mV steps to the films of compounds. The data for dc conductivity were acquired using Keithley model 617 programmable electrometer. Ac conductivity and impedance spectra (IS) measurements were performed using Keithley model 3330 LCZ meter in the frequency range of 4×10^{-2} –100 kHz. All the electrical measurements were performed in the temperature range of 295–523 K in vacuum ($<10^{-3}$ mbar) in dark. The temperature was measured using Chromel–Alumel thermocouple. Both dc and ac conductivity data were recorded using an IEEE-488 data acquisition system.

Synthesis

4-(2- $\{ (E)-[(2E)-(phenylmethylidene)hydrazono]methyl\}$ phenoxy)phthalonitrile (**3**)

To a solution of 4-nitrophthalonitrile (**2**) (2 g, 11.55 mmol) in dry DMF (20 mL) compound (**1**) (2.59 g, 5.78 mmol) was added and the temperature was increased up to 55 °C. Finely powdered dry K_2CO_3 (1.60 g, 11.60 mmol) was added to the system in eight equal portions at 15 min intervals with efficient stirring and the reaction system was stirred at the same temperature for 5 days. The reaction mixture was poured into ice-water and the precipitate was filtered and dried in vacuum over P_2O_5 . The raw product purified by crystallization from acetone/ethanol solvent system. Yield 2.8 g (69%). Anal. calc. for $\text{C}_{22}\text{H}_{14}\text{N}_4\text{O}$: C, 75.42; H, 4.03; N, 15.99; Found: C, 75.01; H, 4.31; N, 15.75. IR (KBr tablet) $\nu_{\text{max}}/\text{cm}^{-1}$: 3047 $\nu(\text{Ar}-\text{CH})$, 2984 $\nu(\text{alip}-\text{CH})$, 2229 ($\text{C}=\text{N}$), 1618–1600 ($\text{C}=\text{C}$), 1555 $\nu(\text{CH}=\text{N})$, 1275–1247 $\nu(\text{C}-\text{O}-\text{C})$, 980 $\delta(\text{CH})$. ^1H NMR (DMSO- d_6), (δ : ppm): 8.45 (s, 1H, $\text{CH}=\text{N}$), 8.35 (s, 1H, $\text{CH}=\text{N}$), 7.92–7.88 (d, 2H, ArH), 7.72–7.57 (m, 4H, ArH), 7.45–7.40 (d, 2H, ArH), 7.15–7.01 (m, 4H, ArH). ^{13}C NMR (DMSO- d_6), (δ : ppm): 165.45, 162.13, 160.51, 158.11, 141.12, 138.78, 136.62, 134.15, 133.42, 130.92, 128.18, 124.77, 122.19, 121.54, 120.35, 120.03, 118.85, 116.44, 115.78, 112.44, 108.12. MS (ESI), (m/z): Calculated: 350.12; Found: 351.25 $[\text{M}+\text{H}]^+$.

Synthesis of phthalocyanines (**4–6**)

In a glass sealed tube, the mixture of compound **3** (0.20 g, 0.571 mmol), dry N,N-dimethylaminoethanol (DMAE, 3 mL), 1,8-diazabicyclo[5.4.0] undec-7-ene (DBU, 3 drops) and for metallophthalocyanines (**5**, **6**) stoichiometric amounts of related anhydrous metal salts ($\text{Zn}(\text{CH}_3\text{COO})_2$; NiCl_2) were heated to 150 °C for 24 h. Then the green products were precipitated by addition of methanol and filtered.

Metal-free phthalocyanine (4). The dark green solid product was purified by column chromatography with chloroform:methanol (100:0.5) as eluent. Yield: 46 mg (22%), mp > 300 °C. Anal. calc. for $\text{C}_{88}\text{H}_{58}\text{N}_{16}\text{O}_4$: C, 75.31; H, 4.17; N, 15.97; Found: C, 75.59; H, 4.48; N, 15.52. IR (KBr tablet) $\nu_{\text{max}}/\text{cm}^{-1}$: 3281 ($-\text{NH}$), 3045 $\nu(\text{Ar}-\text{CH})$, 2982 $\nu(\text{alip}-\text{CH})$, 1615–1597 ($\text{C}=\text{C}$), 1550 $\nu(\text{CH}=\text{N})$, 1270–1255 $\nu(\text{C}-\text{O}-\text{C})$, 973 $\delta(\text{CH})$. ^1H NMR (DMSO- d_6), (δ : ppm): 8.41 (bs, 8H, $\text{CH}=\text{N}$), 7.82–7.60 (m, 24H, ArH), 7.35–7.28 (m, 12H, ArH), 7.11–6.98 (m, 12H, ArH). UV–Vis (CHCl_3) $\lambda_{\text{max}}/\text{nm}$: $[(10^{-5} \text{ } \epsilon, \text{ dm}^3 \text{ mol}^{-1} \text{ cm}^{-1})]$. 699 (5.07), 660 (5.03), 640 (4.77) 604 (4.59), 338 (5.12). MS (ESI), (m/z): Calculated: 1402.48, Found: 1403.95 $[\text{M}+\text{H}]^+$.

Synthesis of zinc (II) phthalocyanine (5). Eluent for column chromatography: chloroform:methanol (100:1). Yield: 80 mg (39.1%), mp > 300 °C. Anal. calc. for $\text{C}_{88}\text{H}_{56}\text{N}_{16}\text{O}_4\text{Zn}$: C, 72.05; H, 3.85; N, 15.28; Found: C, 72.52; H, 4.11; N, 15.11. IR (KBr tablet) $\nu_{\text{max}}/\text{cm}^{-1}$: 3057 $\nu(\text{Ar}-\text{CH})$, 2995 $\nu(\text{alip}-\text{CH})$, 1620–1602 ($\text{C}=\text{C}$), 1561 $\nu(\text{CH}=\text{N})$, 1272–1247 $\nu(\text{C}-\text{O}-\text{C})$, 985 $\delta(\text{CH})$. ^1H NMR (DMSO- d_6), (δ : ppm): 8.55–8.42 (bd, 8H, $\text{CH}=\text{N}$), 8.02–7.73 (m, 24H, ArH), 7.42–7.33 (m, 12H, ArH), 7.21–7.08 (m, 12H, ArH). UV–Vis (CHCl_3) $\lambda_{\text{max}}/\text{nm}$: $[(10^{-5} \text{ } \epsilon, \text{ dm}^3 \text{ mol}^{-1} \text{ cm}^{-1})]$. 682 (5.25), 620 (4.54), 341

(5.07). MS (ESI), (m/z): Calculated: 1464.40, Found: 1465.93 $[M+H]^+$.

Synthesis of nickel (II) phthalocyanine (6). Eluent for column chromatography: chloroform:methanol (100:1). Yield: 26 mg (28%), mp > 300 °C. Anal. calc. for $C_{88}H_{56}N_{16}O_4Ni$: C, 72.38; H, 3.87; N, 15.35; Found: C, 72.25; H, 3.99; N, 15.51. IR (KBr tablet) ν_{max}/cm^{-1} : 3053 $\nu(Ar-CH)$, 2991 $\nu(alip-CH)$, 1625–1604 (C=C), 1559 $\nu(CH=N)$, 1270–1248 $\nu(C-O-C)$, 981 $\delta(CH)$. 1H NMR (DMSO- d_6), (δ : ppm): 8.35 (bs, 8H, CH=N), 7.92–7.45 (bm, 36H, ArH), 7.25–7.12 (m, 12H, ArH). UV-Vis ($CHCl_3$) λ_{max}/nm : [$(10^{-5} \epsilon, dm^3 mol^{-1} cm^{-1})$]. 673 (5.22), 613 (4.77), 334 (5.14). MS (ESI), (m/z): Calculated: 1458.40, Found: 1481.95 $[M+Na]^+$.

Results and discussion

Synthesis and spectroscopic characterization via complementary techniques

The synthesis route of the novel phthalonitrile (**3**) and phthalocyanine compounds (**4–6**) was shown in Fig. 1. Synthesis of phthalonitrile derivatives can be performed by nucleophilic aromatic substitution reaction based on the reaction of 4-nitrophthalonitrile and a nucleophilic compound in the presence of potassium carbonate. Dipolar aprotic solvents such as DMF, DMSO are used in the reactions. Synthesis of the initial phthalonitrile derivative (**3**) was performed according to literature [25] by the reaction of 4-nitrophthalonitrile and 2-((*E*)-[(2*E*)-(phenylmethylidene)hydrazono]methyl)phenol in DMF and at 55 °C. Potassium carbonate was used as basic catalyst at slightly more than the stoichiometric amount. The compound (**3**) was recrystallized in acetone/ethanol solvent system and pale yellow product was obtained with moder-

ate yield. Spectral data coherent with the proposed structure were obtained. According to the IR spectral results of the compound (**3**), characteristic nitrile stretching vibration was observed at $2229 cm^{-1}$. In 1H NMR spectrum of (**3**), the disappearance of the OH peak of (**1**) and presence of additional aromatic protons indicated that nucleophilic aromatic nitro displacement was accomplished. In ^{13}C NMR of (**3**), the new peaks at 116.44 ppm and 115.78 ppm belonging to nitrile carbons indicated that the nucleophilic aromatic substitution has occurred. Mass spectrum of compound (**3**) indicated that target compound successfully prepared. Stable molecular ion $[M+H]^+$ peak is seen at 351.25 in mass spectrum of the compound (**3**). Also elemental analysis data of compound (**3**) was satisfactory.

Although there are a variety of methods in the literature for the preparation of phthalocyanines [30–33], cyclotetramerization of substituted phthalonitrile or 1,3-diimino-1*H*-isoindoles are most preferred methods for the preparation of phthalocyanine compounds [14,34]. Substituted peripherally or non-peripherally phthalocyanines are prepared from 4-substituted or 3-substituted phthalonitriles by means of cyclotetramerization. This reaction results in the formation of four different isomers products (C_{4h} , C_{2v} , C_s and D_{2h}).

In the present work, 4-substituted phthalonitrile (**3**) was used as initial compound for synthesis of the metal free- and metallo-phthalocyanines (Zn, Ni) and did not make an effort to separate the isomeric mixture. Characterization of new phthalocyanines were performed by IR, 1H NMR, mass spectrometry, UV-Vis spectroscopy and elemental analysis. Spectral results of prepared structures supported the proposed structures. In IR spectra of the phthalocyanines, absence of the nitrile stretching vibration at $2229 cm^{-1}$ indicate that proposed structure of the phthalocyanines were correct. The most important difference between metal free

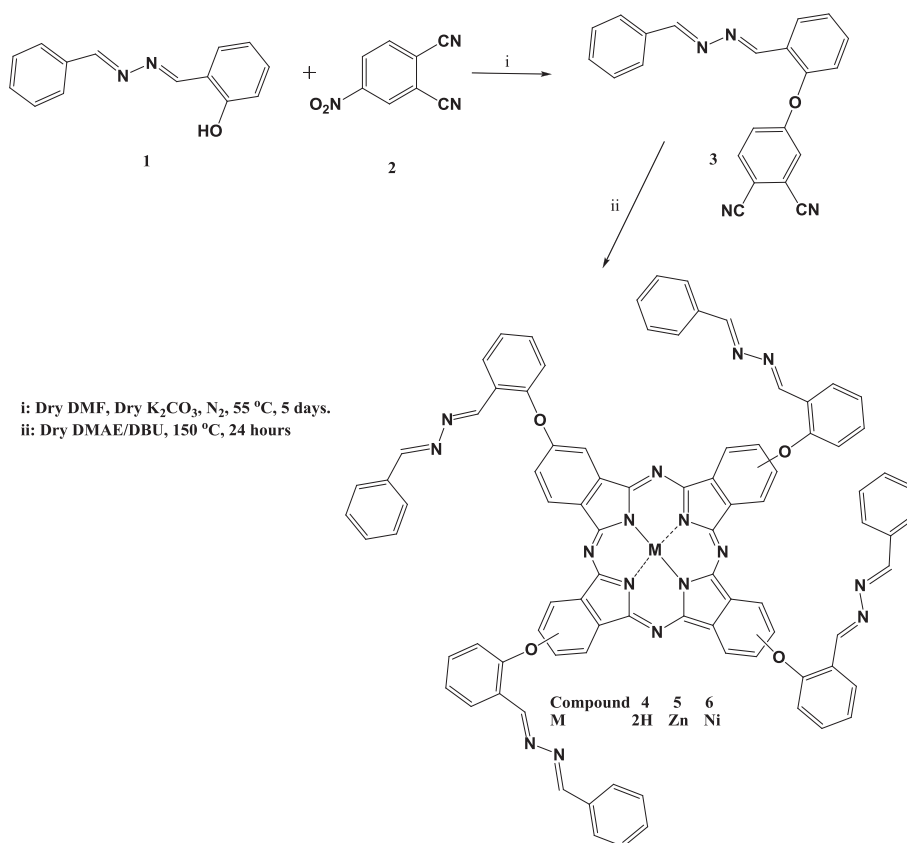


Fig. 1. Synthetic route of novel phthalocyanine compounds.

and metallo phthalocyanines is the inner core —NH vibration observed at 3281 cm^{-1} in the IR spectrum of metal free phthalocyanine (**4**). Other spectral results similar to initial phthalonitrile derivative (**3**).

In the ^1H NMR spectra of the metal free, Zn and Ni Pcs (**4–6**) were obtained in DMSO at room temperature. All protons were observed at aromatic region and the spectra were very similar. The strong aggregation between the metal free phthalocyanine molecules at NMR measurement concentration prevented the observation of inner core protons in ^1H NMR spectrum [35]. In addition, mass spectral results and elemental analysis data of the compounds (**4–6**) were good correlation with proposed structure.

UV–Vis absorption spectra

All phthalocyanine compounds were soluble in organic solvents such as chloroform, THF, dichloromethane, DMF, DMSO and pyridine. All UV–Vis measurements were made in chloroform and at $1 \times 10^{-5}\text{ M}$ concentrations. For metal free phthalocyanine (**4**) the Q band caused by the transitions from π to π^* was observed as doublet at 695 and 660 nm, evidence of non-degenerate D_{2h} symmetry (Fig. 2). Differently from metal free phthalocyanine (**4**), the Q bands of the metallo phthalocyanines (**5**, **6**) were observed at 682 and 673 nm respectively (Fig. 3) and observed as singlet due to D_{4h} symmetry of the metallophthalocyanines. These shift between the Q-bands of Zn(II)Pc (**5**) and Ni(II)Pc (**6**) is in accordance with previous literatures [36,37]. The shoulders of the metal free phthalocyanine (**4**), Zn(II)Pc (**5**) and Ni(II)Pc (**6**) were observed at 640, 620 and 613 nm, respectively. For Q band regions of phthalocyanines, the longer wavelength absorptions are due to the monomeric species and shorter wavelength absorptions (shoulders) are due to the aggregated species [38]. So, in chloroform at $1 \times 10^{-5}\text{ M}$ concentration, monomeric behavior of phthalocyanines (**4–6**) were proved by the dominance and the sharpness of the longer wavelength absorptions. The B bands of the compounds (**4–6**) arising from deeper π levels to LUMO were observed at 338, 341 and 334 nm, respectively (Figs. 2 and 3).

Electrical properties

Dc properties

Dc conductivity measurements of the films of the compounds **4**, **5**, and **6** were done in home-made aluminum chamber at different temperatures in the temperatures range of 295–523 K in vacuum ($<10^{-3}\text{ mbar}$) in dark. Current values passing through the films were recorded versus applied voltages (between -1 and 1 voltage sweep with 50 mV increments) during heating process (I – V

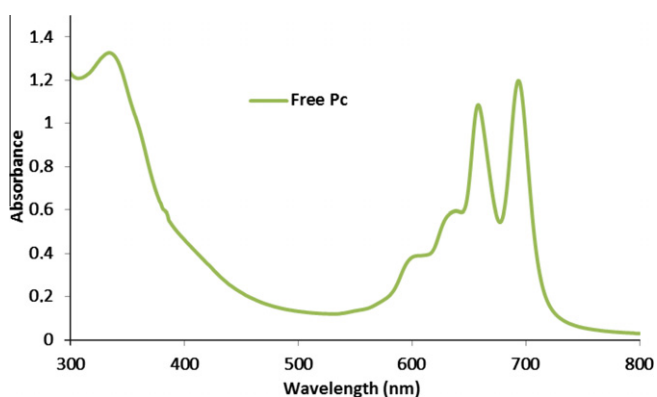


Fig. 2. Absorption spectrum of the metal-free Pc **4** in chloroform at $1 \times 10^{-5}\text{ M}$ concentration.

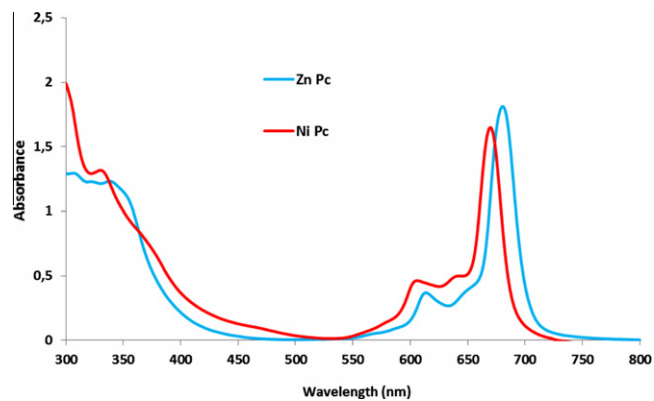


Fig. 3. Absorption spectra of the Zn(II)Pc **5** and Ni(II)Pc **6** in chloroform at $1 \times 10^{-5}\text{ M}$ concentration.

curves). Dc conductivity of the deposited films on IDT was determined using Eq. (1) and the slope of the I – V curves.

$$\sigma_{dc} = \left(\frac{I}{V}\right) \left(\frac{d}{(2n-1)lh}\right) \quad (1)$$

where (I/V) is slope of the I – V graph, d is distance between the finger pair, n is number of the finger pair, l is overlap length and h is thickness of the electrodes.

Fig. 4a and b shows I – V curves of the films of the compounds **4** and **6**, during negative to positive and positive to negative voltage sweeps. As seen from Fig. 4, during negative to positive sweep, current values at zero voltage are greater than the values during positive to negative sweep. Additionally, hysteresis increased as temperature increased. This behavior probably arises from deep

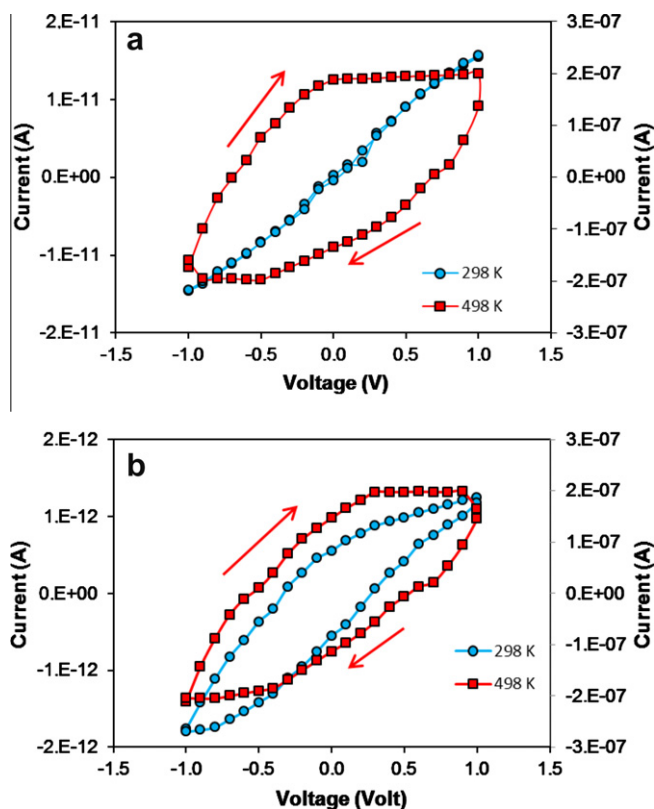


Fig. 4. I – V curves at the temperatures 298 K and 498 K for the (a) film of the compound **4** and (b) film of the compound **6**.

traps. The processes require greater time constant for charging and discharging process. Similar hysteresis was reported earlier [39]. Some parameters such as voltage sweep speed, deep trap level affects hysteresis. The hysteresis at high temperatures suggests that is due to the formation of space charge polarization in the film. Hysteresis effect was also observed for the film of the compound **5**.

Conductivity of the films of the compounds **4**, **5** and **6** was found as 1.0×10^{-9} S/cm, 1.5×10^{-10} S/cm and 1.7×10^{-10} S/cm at 295 K, respectively. The conductivity values increased to 8.5×10^{-6} S/cm, 9.5×10^{-6} S/cm, 1.3×10^{-5} S/cm at 523 K, respectively. Experimental results showed that temperature dependence of the conductivity data of the films obeys Eq. (2) indicating that the compounds **4**, **5** and **6** are semiconductors. The linear relation also shows that the compounds behave as an intrinsic semiconductor in the temperature range of 295–498 K. After 498 K, a small decrease was observed in conductivity of the films. It is well known that, structural/compositional lattice defects increases the localized states and that affects dc conductivity. The change in conductivity behavior with inverse of temperature after 498 K for the films may attributed to the occurrence of a phase transition or presence of different crystallographic phases [40,41]. Calculated dc conductivity values of the films of the compounds **4**, **5** and **6** exhibited same order of conductivity values with other reports in different phthalocyanine films [42]. The temperature dependence of the dc conductivity can be expressed by well-known Arrhenius equation (Eq. (2))

$$\sigma_{dc} = \sigma_0 \exp\left(\frac{-E_A}{kT}\right) \quad (2)$$

where E_A is activation energy, T is temperature, k is Boltzmann's constant and σ_0 is a pre-exponent factor of dc conductivity. Activation energy values of the films were calculated from slope of the straight portions of the Arrhenius plot ($\ln \sigma_{dc} - 1/T$ curves). The values were found as 0.70 eV, 0.91 eV and 0.93 eV for the films of the compounds **4**, **5** and **6**, respectively. Our activation energy values were also exhibited nearly same order of activation energy values with other reports in different phthalocyanine films such as 0.6–0.9 eV [43,44].

Ac properties

AC conductivity measurements. Ac conductivity measurements of the films the compounds **4**, **5** and **6** were done in home-made aluminum chamber at different temperatures in the temperatures range of 295–523 K in vacuum ambient ($<10^{-3}$ mbar) in dark. Ac conductivity measurements were performed in the frequency range of 4×10^{-2} –100 kHz. Frequency dependence of ac conductivity for the film the compound **6** at different temperatures (295–523 K) was presented in Fig. 5. It is clearly seen that ac

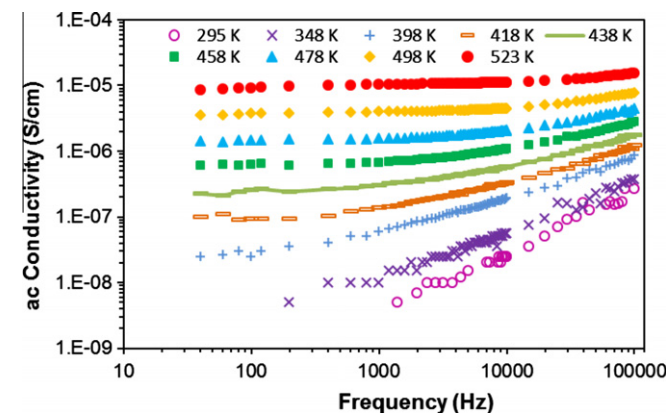


Fig. 5. Frequency dependence of ac conductivity of the film of the compound **6** between the temperatures of 295–523 K.

conductivity (σ_{ac}) of the film increases with increasing temperature. However, temperature dependence of ac conductivity of the film can be analyzed in two parts as low temperature region ($T < \sim 438$ K) and high temperature region ($T > \sim 438$ K). In low temperature region ($T < \sim 438$ K), conductivity of the film strongly depends on frequency and increases with increasing frequency.

In high temperature region ($T > \sim 438$ K), frequency dependence of ac conductivity of the film decreases in the measured frequency range. At all temperatures frequency dependence of the measured ac conductivity of the films obeys the universal power law. The universal power law is given by the Eq. (3) [45].

$$\sigma_{ac} = A\omega^s \quad (3)$$

where ω is the angular frequency, A and s are material depended constants. To gain more information on the charge transport mechanism taking place in the films, the variation of the exponent s with temperature were examined. s values were calculated from slope of straight portions of the σ_{ac} versus ω plot.

Calculated values of s for the films of the compound **4**, **5** and **6** are around 1.0 at 295 K and decreases to 0.2 at 523 K in the frequency range of $\omega > 10$ kHz. The variation of the s values of the film the compound **6** with temperature in high frequency region (>10 kHz) and in low frequency region (≤ 10 kHz) was given in Fig. 6a and of the films the compounds **4**, **5** and **6** in high frequency region in Fig. 6b. As seen from Fig. 6, s values decrease with increasing temperature.

In the band theory, the ac conductivity does not depend on frequency and drops at sufficiently high frequency. In the hopping model the electrons in charged defect states hop over the coulomb barrier. Ac conductivity increases with frequency in this model under the condition that, the frequency exponent $s \leq 1$ [46]. In Correlated Barrier Hopping (CBH) model [46] ac conductivity (first order approximation) is given by following equation:

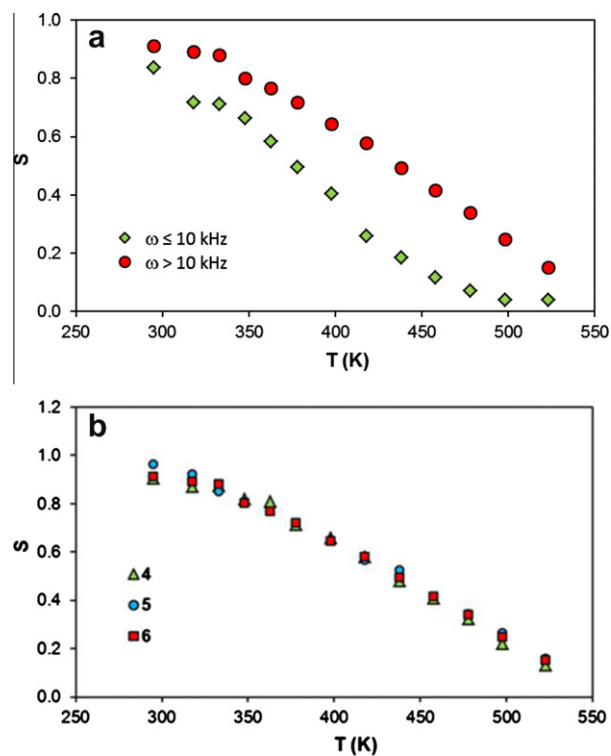


Fig. 6. Temperature dependence of exponents: (a) for the film of the compound **6** in high frequency and low frequency region and (b) for the films of the compounds **4**, **5** and **6** in high frequency region.

$$\sigma_{ac} = \frac{1}{24} n\pi^2 N^2 \varepsilon \varepsilon_0 \omega R_{\omega}^6 \quad (4)$$

where N is the spatial density of defect states, ε and ε_0 are dielectric constants of the materials and free space, respectively, $n = 1$ for a single electron $n = 2$ for hopping of two electrons and R_{ω} is the hopping distance.

The model developed by Elliot (The CBH model), [46,47], suggests a temperature-dependent s value which is given by following equation:

$$s = 1 - \beta = 1 - \frac{6k_B T}{W_m} \quad (5)$$

where k_B is Boltzmann's constant and W_m is the binding energy and T is temperature. In this model s values decreases with increasing temperature. Our results showed that s is a function of temperature for all the films and shows a general tendency to decrease with increasing temperature over the measured frequency and temperature range. The variation of s with temperature and the variation of ac conductivity with frequency (Figs. 5 and 6) are in agreement with the prediction of the hopping model. The same type of temperature dependence for s was observed in other reports in different phthalocyanine films [29]. The quantum-mechanical tunneling (QMT) model [48], predicts an increase in s with temperature or independent of temperature or almost equal to 0.8. In the overlapping-large polaron tunneling (QLPT) model [47], s values depends on frequency and decreases with increasing temperature to a minimum value at a certain temperature, then it increases with increasing temperature. Because of this the models QMT and QLPT are not applicable to our results. The small polaron quantum mechanical tunneling (SP) model predicts an increase in s with increasing temperature. [46,47]. According to these models, we can conclude that charge transport mechanism of the films the compounds **4**, **5** and **6** can be modeled by hopping all over the measured frequency and temperature range.

Impedance measurements. The ac electrical behavior of the films was also characterized by complex impedance spectroscopy technique. In this technique a sinusoidal signal at some frequency are applied to the material and response of the material (impedance data) are measured. A number of such measurements depending on frequency and temperature form the response of the material known as impedance data. The impedance data were represented by $-Z''(\omega)-Z'(\omega)$ curves in complex plane commonly called the Cole–Cole plot (Nyquist plot), where $Z'(\omega)$ is real component of impedance and $Z''(\omega)$ imaginary component of impedance. Nyquist plot for the film the compound **4** was presented in Fig. 7 at indicated temperatures (in Fig. 7b, x-axis and y-axis was not drawn in the same scale to show behavior of the curves).

By examining Fig. 7a the impedance spectra can be characterized by the semicircular shaped arcs suggesting pure capacitive behavior. The curves can be modeled by a resistor parallel with a capacitor in series with another resistor [49]. The films the compounds **5** and **6** also showed same behavior at the temperatures $T < 458$ K.

Fig. 7b shows impedance spectra for film the compound **4** at the temperatures $T \geq 458$ K. By examining Fig. 7a and b, we can say that the curves (in semicircular shaped arc form) in Fig. 7a transforms into full semicircles as in the Fig. 7b with increasing temperature for the film of the compound **4**. With the examination of the Fig. 7b the effect of the temperature on impedance spectra can be seen clearly. Impedance spectra consist of depressed semicircles with different radius, additionally, the radius of the semicircle decreases with increasing temperature. Peak frequency of the complete semicircle, ω_p , satisfies $\omega_p \tau_D = 1$. Where τ_D is time constant [49]. An ideal semicircle in complex plane only appears in Debye dispersion relations for single-relaxation time process. In this case,

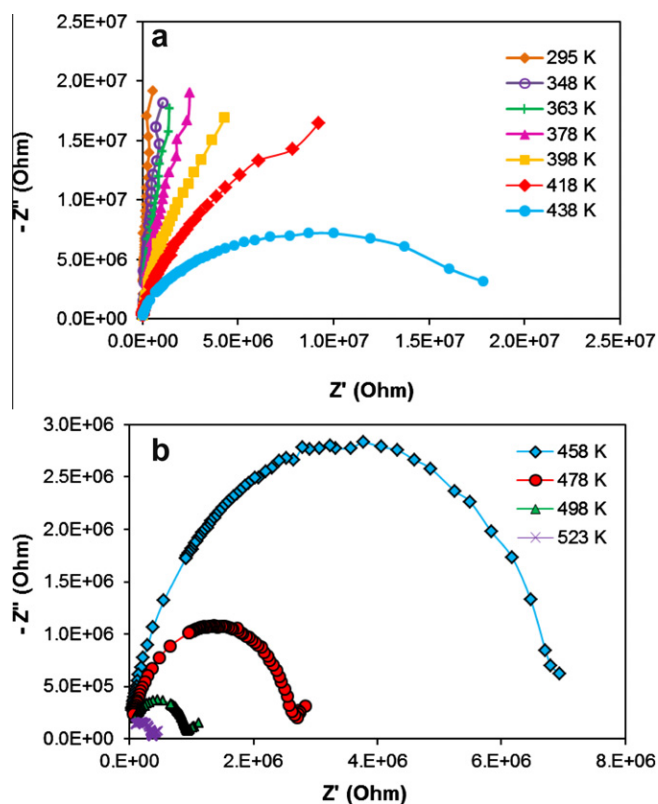


Fig. 7. The Cole–Cole plot for the film of the compound **4** at temperatures: (a) $T < 458$ K and (b) $T \geq 458$ K.

the relaxation time is considered as a distribution of values, rather than a single relaxation time [50]. The depressed semicircles with different radius indicate deviation from Debye dispersion relation. Therefore, the equivalent circuit is modified to include a constant phase element (CPE). The series resistance in the equivalent circuit represents the ohmic losses in the experimental set-up and sheet resistance of the electrode. The parallel resistance is the bulk resistance of the coating material. The intercepts of the semicircular arcs with real axis give us information of the bulk resistance of the compounds. From Fig. 7, it is observed that bulk resistance decreases with increasing temperature indicating semiconductor property. A monotonic decrease in this resistance suggests that the increase of temperature lower the barrier for charge transport. At the temperatures 478 K and 498 K, a straight line was also observed in low frequency region (Fig. 7b). The straight line in the low frequency region indicates the presence of Warburg component [51]. The complex impedance spectrum of the films the compounds **5** and **6** at the temperatures $T \geq 458$ K was similar to those in Fig. 7b.

The variation of imaginary parts of impedance with frequency (ω) for the films of the compounds **4**, **5** and **6** was also investigated. The $-Z''-\omega$ curves for the film of the compound **5** in the temperature range of 295–523 K and at high temperatures were presented in Fig. 8. At low temperatures, $-Z''$ decreases with increasing frequency, and as frequency approaches to 100 kHz frequency dependence of the impedance quite decreases (Fig. 8a). This behavior indicates that there is no current dissipation at these temperatures. At high temperatures, three different remarkable behaviors were observed. (i) The peaks of the imaginary part of the films were observed. As the temperature increases the curves exhibit peaks at different frequencies. This behavior may be an evidence for the occurrence of different electrical relaxation times in the film. (ii) Broadening of the curves was observed with increasing

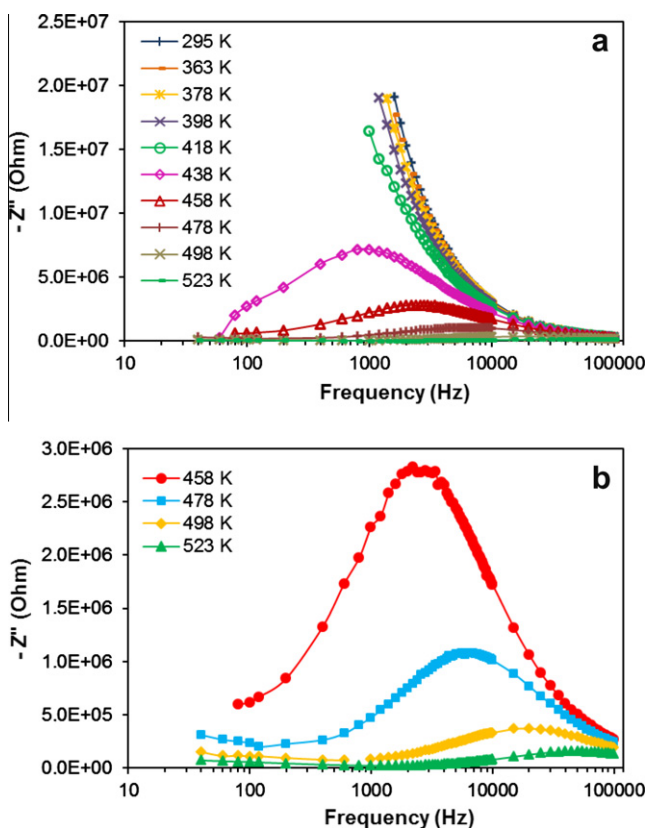


Fig. 8. Variation of imaginary part of impedance with frequency for the film of the compound 5: (a) $295\text{ K} \leq T \leq 523\text{ K}$ and (b) $T \geq 458\text{ K}$.

temperature. This behavior also suggests the presence of an electrical process with a spread of relaxation times, depending on the temperature. (iii) The peak frequencies shifted towards high frequencies for the film of the compound 5.

The $-Z''-\omega$ curves for the films the compounds 4 and 6 were similar to that of film the compound 5 in the temperature range of 295–523 K.

Conclusion

In the presented work, the syntheses of new aldazine substituted metal free, zinc(II) and nickel(II) phthalocyanines were described and these new complexes were characterized by elemental analysis, FT-IR, ^1H NMR, electronic spectroscopy and mass spectra and addition to these techniques for substituted phthalonitrile ^{13}C NMR have been used. Temperature dependence of the conductivity data of the films indicates that the compound of 4, 5 and 6 are semiconductors. The calculated activation energy values were found as 0.70 eV, 0.91 eV and 0.93 eV for the films of 4, 5 and 6, respectively. By examining ac measurement results, charge transport mechanism of the films can be modeled by hopping all over the measured frequency and temperature range. From impedance spectra results, it is observed that bulk resistance of all the compounds decreases with increasing temperature indicating semiconductor property. The result also supports the dc measurement results.

Acknowledgement

The authors thank to The Research Fund of Karadeniz Technical University, Projects No: 2010.111.002.8 (Trabzon/Turkey).

References

- [1] C.C. Leznoff, A.B.P. Lever (Eds.), *Phthalocyanines Properties and Applications*, vol. 1, VCH Publisher, New York, 1989.
- [2] V. Parra, M. Bouvet, J. Brunet, M.L. Rodríguez-Méndez, J.A. Saja, *Thin Solid Films* 516 (2008) 9012–9019.
- [3] M. Bouvet, *Anal. Bioanal. Chem.* 384 (2006) 366–373.
- [4] C.C. Leznoff, A.B.P. Lever (Eds.), *Phthalocyanines Properties and Applications*, Vol. 3, VCH Publishers, New York, 1993.
- [5] G. De La Torre, P. Vazquez, F. Aguillo-Lopez, T. Torres, *J. Mater. Chem.* 8 (1998) 1671–1683.
- [6] F. Yang, S.R. Forrest, *Am. Chem. Soc. Nano* 2 (2008) 1022–1032.
- [7] S.R. Forrest, *Chem. Rev.* 97 (1997) 1793–1896.
- [8] A. Bilgin, B. Ertem, Y. Gök, *Polyhedron* 24 (2005) 1117–1124.
- [9] C.C. Leznoff, A.B.P. Lever (Eds.), *Phthalocyanines Properties and Applications*, vol. 2, VCH Publisher, New York, 1993.
- [10] M. Emmelius, G. Pawlowski, H.W. Vollmann, *Angew. Chem. Int. Ed.* 28 (1989) 1445–1471.
- [11] C.C. Leznoff, A.B.P. Lever (Eds.), *Phthalocyanines, Properties and Applications*, vol. 4, VCH, New York, 1996.
- [12] F. Yılmaz, M. Özer, I. Kani, Ö. Bekaroglu, *Catal. Lett.* 130 (2009) 642–647.
- [13] I. Rosenthal, *Photochem. Photobiol.* 53 (1991) 859–870.
- [14] İ. Degirmencioglu, R. Bayrak, M. Er, K. Serbest, *Dyes Pigm.* 83 (2009) 51–58.
- [15] M. Kandaz, A.T. Bilgiçli, A. Altındal, *Synth. Met.* 160 (2010) 52–60.
- [16] I.N. Tretyakova, V.Ya. Chernii, L.A. Tomachynski, S.V. Volkov, *Dyes Pigm.* 75 (2007) 67–72.
- [17] G. Gümrükçü, M.Ü. Özgür, A. Altındal, A.R. Özkaya, B. Salih, Ö. Bekaroglu, *Synth. Met.* 161 (2011) 112–123.
- [18] J.H. Kiefer, Q. Zhang, R.D. Kern, J. Yao, B. Jursic, *J. Phys. Chem.* 101 (1997) 7061–7073.
- [19] I. Alkorta, F. Blanco, J. Elguero, *Arkivoc* 7 (2008) 48–56.
- [20] I. Picon-Ferrer, F. Hueso-Urena, N.A. Illan-Cabeza, S.B. Jimenez-Pulido, J.M. Martinez-Martos, M.J. Ramirez-Exposito, M.N. Moreno-Carretero, *J. Inorg. Biochem.* 103 (2009) 94–100.
- [21] G. Gürkök, T. Coban, S. Suzen, *J. Enzym Inhib. Med. Chem.* 24 (2009) 506–515.
- [22] G. Gürkök, N. Altanlar, S. Suzen, *Chemotherapy* 55 (2009) 15–19.
- [23] V.B. Kurteva, S.P. Simeonov, M. Stoilova-Disheva, *Pharmacol. Pharm.* 2 (2011) 1–9.
- [24] J. Jayabharathi, V. Thanikachalam, A. Thangamani, M. Padmavathy, *Med. Chem. Res.* 16 (2007) 266–279.
- [25] R. Bayrak, H.T. Akçay, M. Pişkin, M. Durmuş, İ. Degirmencioglu, *Dyes Pigm.* 95 (2012) 330–337.
- [26] D.D. Perrin, W.L.F. Armarego, *Purification of Laboratory Chemicals*, Pergamon, Oxford, 1989.
- [27] M. Godara, R. Maheshwari, S. Varshney, A.K. Varshney, *J. Serb. Chem. Soc.* 72 (2007) 367–374.
- [28] G.J. Young, W. Onyebuagu, *J. Org. Chem.* 55 (1990) 2155–2159.
- [29] E. Yabaş, M. Sülü, S. Saydam, F. Dumludağ, B. Salih, Ö. Bekaroglu, *Inorg. Chim. Acta* 365 (2011) 340–348.
- [30] H. Uchida, P.Y. Reddy, S. Nakamura, T. Toru, *J. Org. Chem.* 68 (2003) 8736–8738.
- [31] C.S. Marvel, J.H. Rssweiler, *J. Am. Chem. Soc.* 80 (1958) 1197–1199.
- [32] N. Safari, P.R. Jamaat, S.A. Shirvan, S. Shoghpor, A. Ebadi, M. Darvishi, A. Shaabani, *J. Porphyrins Phthalocyanines* 9 (2005) 256–261.
- [33] N.P. Farrell, A.J. Murray, J.R. Thornback, D.H. Dolphin, B.R. James, *Inorg. Chim. Acta* 28 (1978) 144–146.
- [34] O.E. Sielcken, L.A. Van de Kuil, W. Drenth, J. Schoonman, R.J.M. Nolte, *J. Am. Chem. Soc.* 112 (1990) 3086–3093.
- [35] İ. Degirmencioglu, E. Atalay, M. Er, Y. Köysal, Ş. Işık, K. Serbest, *Dyes Pigm.* 84 (2010) 69–78.
- [36] Ü. Demirbaş, R. Bayrak, M. Pişkin, H.T. Akçay, M. Durmuş, H. Kantekin, *J. Organomet. Chem.* 724 (2013) 225–234.
- [37] H.T. Akçay, R. Bayrak, Ü. Demirbaş, A. Koca, H. Kantekin, İ. Degirmencioglu, *Dyes Pigm.* 96 (2013) 483–494.
- [38] R.C. George, M. Durmuş, G.O. Egharevba, T. Nyokong, *Polyhedron* 28 (2009) 3621–3627.
- [39] P.D. Hooper, M.I. Newton, G. McHale, M.R. Willis, *Semicond. Sci. Technol.* 12 (1997) 455–459.
- [40] M.S. Masoud, S.A. El-Enein, E. El-Shereafy, *J. Therm. Anal. Calorim.* 37 (1991) 365–373.
- [41] H. Hassib, A.A. Razik, *Solid State Commun.* 147 (2008) 345–349.
- [42] Z. Odabaş, E.B. Orman, M. Durmuş, F. Dumludağ, A.R. Özkaya, M. Bulut, *Dyes Pigm.* 95 (2012) 540–552.
- [43] R.C. Cherian, C.S. Menon, *J. Phys. Chem. Solids* 69 (2008) 2858–2863.
- [44] Z. Odabaş, F. Dumludağ, A.R. Özkaya, S. Yamauchi, N. Kobayashi, Ö. Bekaroglu, *Dalton Trans.* 39 (2010) 8143–8152.
- [45] M. Pollak, T.H. Geballe, *Phys. Rev.* 122 (1961) 1742–1754.
- [46] S.R. Elliot, *Adv. Phys.* 36 (1987) 135–218.
- [47] A.R. Long, *Adv. Phys.* 31 (1982) 553–637.
- [48] A. Ghosh, *Phys. Rev. B* 41 (1990) 1479–1488.
- [49] E. Barsoukov, J.R. Macdonald, *Impedance Spectroscopy Theory, Experiment and Applications*, second ed., John Wiley & Sons Inc., 2005.
- [50] Y.J. Chen, X.Y. Zhang, T.Y. Cai, Z.Y. Li, *J. Alloys Compd.* 379 (2004) 240–246.
- [51] F. Josse, R. Lukas, R. Zhou, S. Schneider, D. Everhart, *Sens. Actuators B – Chem.* 36 (1996) 363–369.